SAND2016-8394J

^{1}H-^{19}F REDOR-Filtered NMR Spin Diffusion Measurements of Domain Size in Heterogeneous Polymers

Eric G. Sorte[1], Todd M. Alam[1,*]

[1] Department of Organic Material Science, Sandia National Laboratories, Albuquerque, New Mexico 87185, USA

Abstract

Solid state NMR spectroscopy is inherently sensitive to chemical structure and composition, and thus makes an ideal method to probe the heterogeneity of multicomponent polymers. Specifically, NMR spin diffusion experiments can be used to extract reliable information about spatial domain sizes on multiple length scales, provided that magnetization selection of one domain can be achieved. In this paper, we demonstrate the preferential filtering of protons in fluorinated domains during NMR spin diffusion experiments using ^{1}H-^{19}F heteronuclear dipolar dephasing based on rotational echo double resonance (REDOR) MAS NMR techniques. Three pulse sequence variations are demonstrated based on the different nuclei detected: direct ^{1}H detection, plus both ^{1}H→^{13}C cross polarization (CP) and ^{1}H→^{19}F CP detection schemes. This ^{1}H-^{19}F REDOR-filtered spin diffusion method was used to measure fluorinated domain sizes for a complex polymer blend. The efficacy of the REDOR-based spin filter does not rely on spin relaxation behavior or chemical shift differences, and thus is applicable for performing NMR spin diffusion experiments in samples where traditional magnetization filters may prove unsuccessful. This REDOR-filtered NMR spin diffusion method can also be extended to other samples where a heteronuclear spin pair exists that is unique to the domain of interest.

Keywords: NMR, ^{1}H, ^{19}F, ^{13}C, REDOR, spin diffusion, polymer blend, proton exchange membrane

* Corresponding Author: tmalam@sandia.gov, (505) 844-1225

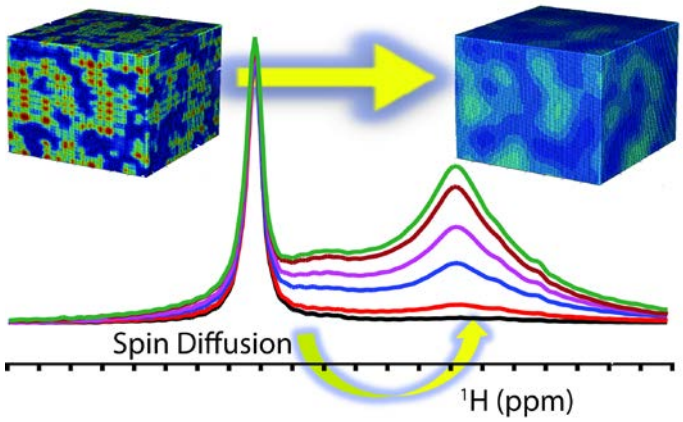

^{1}H-^{19}F REDOR-filtered MAS NMR spin diffusion pulse sequences are introduced that exploit heteronuclear dipole recoupling to preferentially suppress the ^{1}H magnetization in a single chemical domain. We demonstrate the performance of these REDOR-filtered experiments to directly measure the fluorinated domain size in a blended copolymer where relaxation-based filters proved unsuccessful.

Introduction

Many polymers with commercial applications are multi-component systems whose macroscopic properties (such as mechanical stability and conductivity) are determined by their microscopic characteristics, including the sizes of phase-separated domains.[1] Measurement of domain sizes are therefore important for optimizing a polymer's performance in its intended capacity. A variety of techniques have been used to characterize polymer morphology, including spectroscopic methods such as NMR, IR, and Raman,[2-5] microscopic methods such as AFM, SEM and TEM,[4, 6] and scattering methods including SAXS and SANS.[7-10] Using these different techniques, the microscopic properties of multicomponent polymers can be mapped to their functional characteristics allowing optimization of the synthesis and processing steps to maximize the performance critical for a given application.

One important application is the development of polymer proton exchange membranes (PEMs) for different energy storage technologies, including use in fuel cells and[11, 12] conventional[13] and flow batteries.[14] Alternatives to the industry-standard perfluoronated Nafion polymer membrane are consistently being explored to obtain PEMs with increased conductivity and extended high-temperature performance. Recent studies have surveyed a range of sulfonated random and block copolymers to help develop correlations between morphology and conductivity.[6, 15] Blends of common immiscible polymers such as fluoropolymers and polystyrenes allow the combination of both the mechanical and chemical stability of fluorinated polymers with the ionic conductivity of polyelectrolytes. These blends allow for the variable tuning of properties while avoiding the synthetic difficulties associated with creating block and graft copolymers.[16-18] Efforts to optimize membrane conductivity (as well as other properties) and correlate it with the nano-scale morphology depends on a reliable method to measure changes in the domain size during synthetic and processing iterations.

NMR spin diffusion experiments can provide particularly robust domain-size measurements, especially in disordered polymer systems where scattering techniques may fail. In a typical spin diffusion experiment, the ^{1}H magnetization is selectively suppressed (filtered) in one chemical environment, followed by measurement of the magnetization recovery via spin diffusion originating from the strong ^{1}H-^{1}H homonuclear dipolar coupling.[19] The recovered magnetization buildup as a function of the spin diffusion time τ_{SD} then provides a measure of the domain size within the material.[20] A wide variety of polymer systems have been studied with spin diffusion techniques, including blends,[21, 22] fibers,[23] block copolymers,[24] polyurethanes,[25] and semi-crystalline bulk polymers.[26-28] The choice of which pulse sequence to use to filter the ^{1}H magnetization for a targeted domain depends on the chemical composition, relaxation dynamics, and spectral profile of the material in question. For samples with sufficient ^{1}H NMR chemical

shift resolution, variants of CRAMPS-filtered sequences[21, 29] have been used. Double quantum-filtered,[30] dipolar-filtered,[31, 32] and $T_{1\rho}$-filtered[33] sequences exploit homonuclear dipolar couplings to select domains through the creation of multiple quantum coherences or through differences in the transverse relaxation dynamics, while 2D WISE (wideline separation) experiments rely on ^{1}H-^{13}C CP for detecting the spin diffusion process.[34] Sequences incorporating heteronuclear dephasing methods include the HARDSHIP sequence,[35] along with the more recent ^{1}H-^{13}C Lee-Goldburg cross polarization (CPLG) and ^{1}H-^{13}C REDOR "hole-burning" NMR experiments to measure spin-diffusion coefficients.[36-39] In this paper, we extend these REDOR "hole-burning" studies by introducing a ^{1}H-^{19}F REDOR-filtered NMR spin diffusion sequence to measure the size of fluorinated domains in a polymer blend membrane. It is demonstrated that the ^{1}H spin diffusion can be readily measured either using direct ^{1}H detection, or through ^{13}C or ^{19}F detection following cross-polarization from the ^{1}H magnetization.

Experimental

For this paper, we investigated a blended copolymer composed of hydrophilic polyelectrolyte and hydrophobic polyvinylidene (PVDF) components (shown in Scheme 1) compatabilized with tetrabuytlammonium hydroxide (TBA-OH).[40] The polyelectrolyte was a random copolymer of vinylbenzyl sulfonic acid and vinylbenzyl alcohol. The ratio of PVDF to the polyelectrolyte was 65/35 (w/w), and was solvent cast into membranes with a nominal thickness of 25 μm before being activated with 1 M hydrochloric acid. Details of the blended copolymer synthesis are given in a recent paper by Hou *et al.*[40] The hydrated membranes explored here were synthesized by the Madsen group,[40] and used as-received following atmospheric exposure. For the dehydrated membrane experiments, the samples were dried under vacuum over P_2O_5 for 72 hours prior to being packed and sealed in MAS NMR rotors.

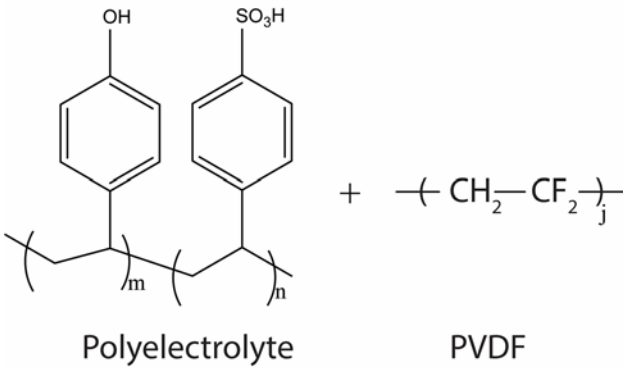

Scheme 1. The chemical structure of the blended PVDF/polyelectrolyte copolymer. The polyelectrolyte component consists of a random copolymer of vinylbenzyl sulfonic acid and vinylbenzyl alcohol. The PVDF polymer contains both crystalline and amorphous phases as discussed in the text.

The ^{1}H-^{19}F REDOR-filtered NMR spin diffusion experiments were carried out on a Bruker Avance III spectrometer at a ^{1}H Larmor frequency of 400.1 MHz. All experiments were performed using a 2.5 mm [^{1}H,^{19}F, X] triple resonance MAS probe, with 20 kHz spinning speeds, 3 s recycle delay, 100 kHz ^{1}H pulses, 80 kHz ^{19}F pulses, 80 kHz ^{13}C pulses, at a sample temperature of 311 K (corrected for frictional heating). A spectral window of 160 kHz was used for the ^{1}H MAS NMR and 150 kHz for the ^{19}F MAS NMR. Time-proportional phase modulation (TPPM) ^{1}H decoupling was used during ^{13}C and ^{19}F acquisition on the ^{1}H channel, while the ^{1}H-^{19}F REDOR portion utilized XY-8 phase cycling. CP contact times were optimized for S/N at 1 ms for both $^{1}H \rightarrow {}^{13}C$ and $^{1}H \rightarrow {}^{19}F$ CP, with 8 K scan averaging for the ^{13}C CPMAS, and 1 K scans for the ^{19}F CPMAS detection schemes. The ^{1}H NMR chemical shifts were referenced to an external secondary H_2O reference (δ = +4.8 ppm) with respect to TMS (δ = 0 ppm), the ^{13}C NMR chemical shifts were referenced to the secondary standard adamantane (δ = +38.0 ppm) with respect to TMS, and the ^{19}F NMR chemical shifts were referenced to the secondary standard ammonium trifluoroacetate (δ = -72 ppm) with respect to $CFCl_3$ (δ = 0 ppm). The DMFIT[41] software was used for all spectral deconvolutions.

Three variations of the ^{1}H-^{19}F REDOR-filter NMR spin diffusion experiment were developed as shown in Figure 1. For situations where the ^{1}H chemical shift resolution of the PVDF phases is sufficient for accurate deconvolution of the source and sink domain resonances, the spin diffusion recovery curves can be measured via direct ^{1}H observation (Figure 1A). For situations where the ^{1}H resonances may not be sufficiently resolved we also demonstrated both ^{1}H-^{13}C (Figure 1B) and ^{1}H-^{19}F (Figure 1C) CPMAS variations for detection using nuclei with greater spectral resolution. Note that for polymers with large domains or slow diffusion constants, long spin diffusion times τ_{SD} would be necessary for complete spin diffusion magnetization recovery. In these situations, spin-lattice T_1 relaxation can mask the spectral changes in the measured spin diffusion data. However, the effects of T_1 relaxation can be somewhat mitigated with appropriate phase cycling (+/-) of the $\pi/2$ pulse just before the spin diffusion period.[20] The signal intensity shown in the magnetization recovery curves presented in the results section have also been empirically corrected for T_1 relaxation effects.

Results and Discussion

Figure 2 shows the deconvoluted ^{1}H MAS NMR (isotropic chemical shift region) and assignment of the PVDF/polyelectrolyte blend. For the partially hydrated polymer membrane (Figure 2A) the narrow resonance near δ = +8.5 ppm results from water, sulfonic acid and alcohol protons in rapid exchange, while the broad resonance at $\delta \sim$ +6 ppm is assigned to aromatic protons of the polyelectrolyte. The low frequency resonance near δ = +2 ppm consist primarily of PVDF protons, with smaller unresolved contributions from the polyelectrolyte vinyl protons. The complete ^{1}H MAS NMR spectrum is provided in the supplemental material (Figure S7) which shows numerous spinning sidebands which clearly demonstrates the aromatic and PVDF regions still have significant ^{1}H-^{1}H dipolar coupling. The ^{1}H MAS NMR spectrum for the dry polymer membrane (Figure 2B) shows that the PVDF, vinyl, and aromatic resonances remain unchanged, while the sharp water resonance disappears and is replace by smaller, but strongly hydrogen-bonded ^{1}H environment near $\delta \sim$ + 11 ppm.

To characterize the PVDF domain size in this PVDF/polyelectrolyte polymer blend, it is desirable to suppress the ^{1}H magnetization in the fluorinated PVDF (sink) phase, followed by a measurement of the NMR spin diffusion magnetization recovery curve as the redistribution of ^{1}H magnetization from the other polymer domains (source domain) occurs. In this polymer blend, there was ^{1}H spectral overlap of the aromatic (+6 ppm) and the PVDF (+2 ppm) resonances even at 20 kHz MAS, making direct chemical shift filtering techniques challenging.

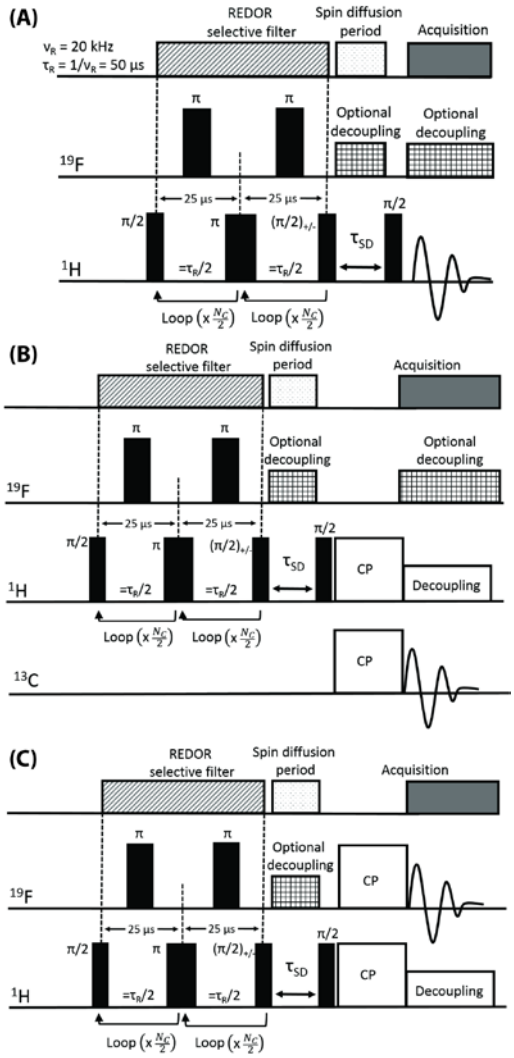

Figure 1. ^{1}H-^{19}F REDOR-filtered NMR spin diffusion pulse sequences utilizing different observe nuclei: (A) direct ^{1}H-observe, B) ^{1}H→^{13}C CP observe, and (C) ^{1}H→^{19}F CP observe. The ^{19}F π pulses were rotor synchronized to refocus the ^{1}H-^{19}F heteronuclear dipole coupling eliminated by MAS, which selectively dephases the ^{1}H magnetization in the PVDF domain. N_c = 26 per acquisition for an echo time of 1.3 ms was used for suppression of the ^{1}H signal in the PVDF phase.

Moreover, the ^{1}H longitudinal spin lattice relaxation times of the aromatic and PVDF domains were roughly equal (T_1 (aromatic) = 1.2 s ≈ T_1 (PVDF) = 1.3 s), precluding the use of T_1-filtering methods. Finally, the transverse relaxation times or line widths (T_2 ~ 1/FWHM) were also not sufficiently different to employ dipolar-filtering for discrimination of the fluorinated domain.

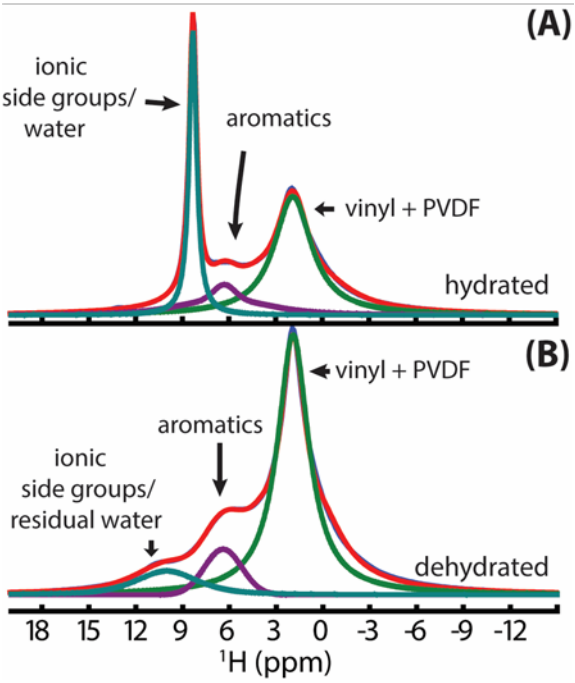

Figure 2. ^{1}H MAS NMR spectra (311 K, ν_R = 20 kHz) of the PVDF/polyelectrolyte blended copolymer showing the deconvolution of the spectral features (isotropic region shown) for A) the hydrated (as-received), and (B) dried polymer membrane. The +2 ppm resonance was assigned to the ^{1}H in PVDF and the polyelectrolyte vinyl, while the +6.3 ppm resonance was assigned to the aromatic ^{1}H environment. The high-frequency resonance at +8.5 ppm results from exchanging protons of water and the ionic sulfonic and alcohol groups which diminishes and shifts to high frequency chemical shift of ~ +11 ppm with dehydration.

In this paper we have introduced the ^{1}H-^{19}F REDOR-filtered REDOR NMR spin diffusion pulse sequence (Figure 1) to obtain a clean discrimination of the protons in the PVDF phase. In the traditional REDOR experiment,[42] the reduced signal S_r results from dephasing produced by recoupling of the heteronuclear dipolar interactions (*i.e.* ^{1}H-^{19}F in the present example) with the introduction of rotor synchronized heteronuclear ^{19}F π pulses. This dephased signal intensity is compared to the full Hahn echo[43] signal S_0 without recoupling,[44, 45] with the ratio related to the heteronuclear second moment M_2 for a multi-spin system using[46, 47]

$$\frac{S_0 - S_r}{S_0} = \frac{4}{3\pi^2}(N_C\tau_R)^2 M_2^{HF} \qquad (1)$$

where the dipolar evolution time $N_C\tau_R$ is the product of the number of rotor cycles N_C and the inverse of the MAS speed ($\tau_R = 1/\nu_R$). M_2^{HF} in turn depends on the effective heteronuclear dipolar coupling constant $\left(d^{HF}\right)$ as

$$M_2^{HF} = \frac{4}{15} 4\pi^2 I(I+1) \sum_j d_j^2$$
$$d^{HF} = \frac{\gamma_H \gamma_F \hbar \mu_0}{8\pi^2 r_{HF}^3}, \quad (2)$$

where γ_H and γ_F are the gyromagnetic ratios of the ^{1}H and ^{19}F nuclei, I is the spin quantum number of the ^{19}F dephasing nucleus, r_{HF} is the inter-nuclear distance, and the summation is over all ^{1}H-^{19}F interactions in the system. Depending on the M_2^{HF} of the fluorinated domain, the signal suppression can be optimized by varying $N_C \tau_R$ following Eq. (1). In a traditional REDOR experiment, $S_0 - S_r / S_0$ is used to provide a measure of d^{HF} or r_{HF} for the sample. For the REDOR-filtered NMR spin diffusion experiments only the dephased signal S_r is of concern, and in our example allows the selective dephasing of the ^{1}H near ^{19}F in the PVDF domain. In the polymer blend sample, optimal suppression was obtained using N_c = 26 ($N_C \tau_R$ = 1.3 ms), which was followed by spin diffusion of ^{1}H magnetization back into the PVDF domain during τ_{SD} (see Figure 1). The domain sizes were evaluated by analyzing the magnetization recovery curve based on integration of PVDF-associated resonances (e.g. ^{1}H, ^{19}F or ^{13}C).

NMR spin diffusion is expected to follow a Fick's Law diffusion process of the form[24]

$$\frac{\partial M(\vec{r}, \tau_{SD})}{\partial t} = \vec{\nabla} \cdot \left[D(\vec{r}) \vec{\nabla} M(\vec{r}, \tau_{SD}) \right], \quad (3)$$

where $M(\vec{r}, \tau_{SD})$ is the spatial magnetization and $D(\vec{r})$ is the domain specific spin diffusion constant. Differential equations of this type have solutions that are proportional to $\sqrt{D\tau_{SD}}$,[20] and thus the magnetization recovery is commonly plotted as a function of $\sqrt{\tau_{SD}}$. Using the DIFFSIM simulation program developed in our lab to analyze NMR spin diffusion data via Eq. (3),[48] the domain sizes were determined assuming a 3D model of randomly dispersed uniform-sized PVDF domains. While T_1 relaxation can also be included during the analytical evaluation of the spin diffusion response, relaxation was not explicitly included for the simulations presented below. The spin diffusion coefficients D for each domain was estimated from analytical expressions for a Gaussian line shape as employed in previous studies[32, 49-51]

$$D = \frac{1}{12} \sqrt{\frac{\pi}{2 \ln 2} \langle r^2 \rangle} \Delta \upsilon_{1/2} \quad (4)$$

where $\sqrt{\langle r^2 \rangle}$ is the mean square distance between the ^{1}H spins (estimated as 0.182 nm in PVDF and 0.249 nm for the aromatic protons in the polyelectrolyte), and $\Delta\upsilon_{1/2}$ is the full-width-at-half-maximum line width. This relationship provides a first-order estimate of the ^{1}H spin diffusion, because the MAS linewidth is principally governed by nearest-neighbor ^{1}H-^{1}H interactions, while longer range interactions can influence the spin diffusion process.[52] Heteronuclear dipole coupling also contributes the ^{1}H linewidths, but the effects of moderate MAS are expected to largely suppress those interactions (see Fig. S5 supplemental material).[33, 52] For the same reasons, ^{19}F effects on the ^{1}H spin diffusion are not expected to make a large contribution. It is possible to incorporate ^{19}F decoupling during the spin diffusion period (Figure 1) if these heteronuclear contributions become significant, but ^{19}F decoupling was not incorporated in the current example. Based on the experimental MAS linewidths (no ^{19}F decoupling) we estimate an effective diffusion constant for the PVDF domain of $D_P = 0.028$ nm^2/ms, and for the aromatic polyelectrolyte phase $D_A = 0.067$ nm^2/ms. The water/ionic protons in the hydrated membrane are expected to have a negligible impact on the observed spin diffusion to the PVDF domain, as the *D* for this mobile environment is very small in comparison to the rigid aromatic protons ($D_{water} < 0.001$ nm^2/ms based on the linewidth in Figure 2A). As reported by other groups, the magnitude of *D* is inversely proportionally to the MAS rate and produces trends that are consistent with the reduction in *D* estimated from the MAS line widths using Eqn. 4.[37, 39, 48, 53-55] Holestein *et al*. reported a ^{1}H spin diffusion value of $D_P = 0.2$ nm^2/ms in PVDF under 10 kHz MAS;[52] making our smaller *D* value reasonable (estimated at 20 kHz MAS). It is well-known that the accurate determination of *D* remains an issue in analyzing NMR spin diffusion experiments, with changes in *D* producing a scaling of the calculated domain size. We argue that the estimated effective *D* based on the MAS line width utilized in the current discussion provides an upper limit to the measured domain size. For many systems, where one is exploring the impact of synthesis or processing on the local morphology, relative changes in the domain size can still be measured directly even with an uncertainty in *D*.

Figure 3 shows the ^{1}H-^{19}F REDOR-filtered NMR spin diffusion spectra (^{1}H detected, Figure 1A) as a function of spin diffusion times τ_{SD} for the PVDF/polyelectrolyte blend. For the hydrated polymer blend (Figure 3A), the ^{1}H signal for the PVDF domains is selectively suppressed for short spin diffusion times ($\tau_{SD} \leq 1$ ms), while the ^{1}H signals from the polyelectrolyte aromatic and ionic $H_2O/SO_3H/OH$ environments remains (black line, Figure 3A). Approximately 10% of the original signal remains in the vinyl+PVDF resonance after dephasing, which we attribute to overlapping vinyl ^{1}H in the polyelectrolyte phase. The aromatic resonance remains largely unaffected. The spectra in Figure 3A are shown normalized to the aromatic resonance to graphically emphasize the magnetization buildup in the PVDF domain, but

this can be slightly deceiving due to differences in the ^{1}H T_1's between polymer environments. For the analysis of the NMR spin diffusion recovery curves, the absolute intensity from deconvolution for the different resonances was employed. With increasing τ_{SD}, the magnetization from the aromatic and vinyl ^{1}H of the polyelectrolyte phase diffuses back into the PVDF domain, until at the longest spin diffusion

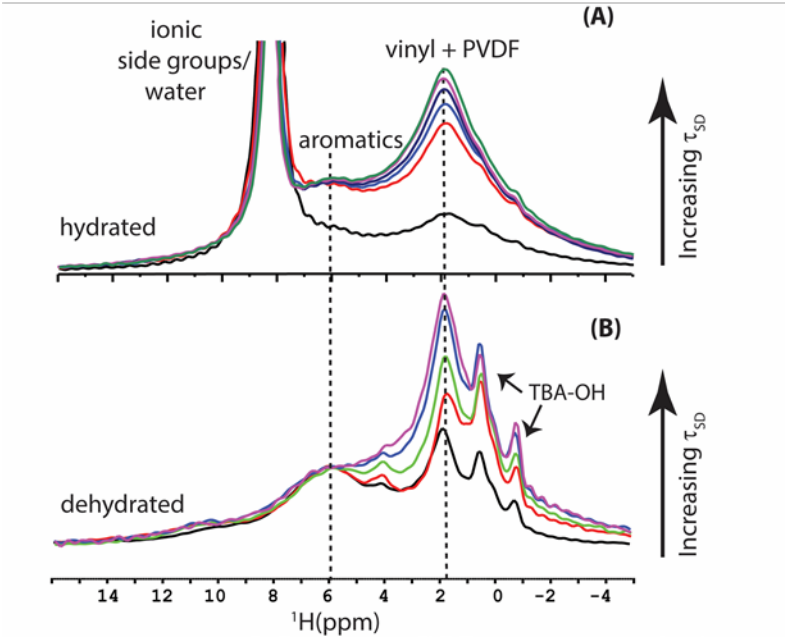

Figure 3: ^{1}H-^{19}F REDOR-filtered ^{1}H-detected MAS NMR spin diffusion spectra as a function of the spin diffusion time τ_{SD} (1 to 200 ms) using the pulse sequence in Figure 1A for the (A) hydrated and (B) dehydrated polymer blend membrane.

times ($\tau_{SD} \geq 200$ ms) the PVDF ^{1}H magnetization has fully recovered (top green line in Figure 3A; compare to Figure 2A). For the dehydrated polymer (Figure 3B), the significant total signal loss during the REDOR filter (~91%) also emphasizes the residual TBA-OH solubilizer due to the long T_2 of TBA (see assignment discussion in supplemental material). This polymer blend membrane, with the multiple overlapping ^{1}H resonances (Figure 3), provides an example where selective filtering of magnetization is not realized by differences in relaxation behavior or chemical shift resolution, but where the ^{1}H-^{19}F REDOR-filter is uniquely useful. This example also highlights the T_2 relaxation limitation of the ^{1}H-^{19}F REDOR filter where significant S/N degradation may occur during the long REDOR period $\left(N_C\tau_R\right)$ used during the complete suppression of the fluorinated domain. The relatively short ^{1}H T_2 in materials may therefore limit the measurement of very large domain sizes. Higher MAS speeds would lead to increased T_2 values, but this improvement would be counteracted by the reduction of the spin diffusion constant *D* (see discussion above). Investigation involving coupling between different heteronuclear spin pairs (*e.g.* ^{31}P-^{13}C,

^{31}P-^{15}N etc.) may produce slower T_2 relaxation, and correspondingly the ability to measure larger domain sizes.

The measured spin diffusion recovery data (open circles) for the hydrated and dehydrated polymer blend are shown in Figure 4A and 4B, respectively. Simulations of these magnetization recovery curves were performed by incrementing the PVDF domain size, while maintaining the constant experimental volume fraction, to minimize χ^2. An average PVDF domain size of 4.0 ± 0.2 nm was determined was measured for both the hydrated and dehydrated domains. The χ^2-minimized best fit to each data set (blue broken line), while two other domain size simulations (solid lines) with their corresponding larger χ^2 values are provided as a demonstration of the sensitivity of the NMR spin diffusion measurements to yield accurate domain sizes on the order of ± 0.2 nm. The impact of ~ 65 to 80% variation in the estimated *D* on the simulated recovery curves is shown in Figure S6, and would produce a similar error in the measured domain size.

While these results are promising, there will be many instances where the ^{1}H NMR signal is insufficiently resolved for accurate spectral deconvolutions. In these cases, it possible to include a ^{1}H→^{13}C CP step to the ^{1}H-^{19}F REDOR-filtered pulse sequence (Figure 1B) for ^{13}C detection to improve the spectral resolution of the different domains. An example for the hydrated PVDF polymer blend membrane is shown in Figure 5A, where the buildup of the PVDF CH_2 resonance is monitored (see supplemental material for full resonance assignments) as shown in Figure 5B (open symbols). Additional ^{1}H-^{13}C and ^{19}F-^{13}C CPMAS NMR experiments used for assignments is provided in the supplemental material.

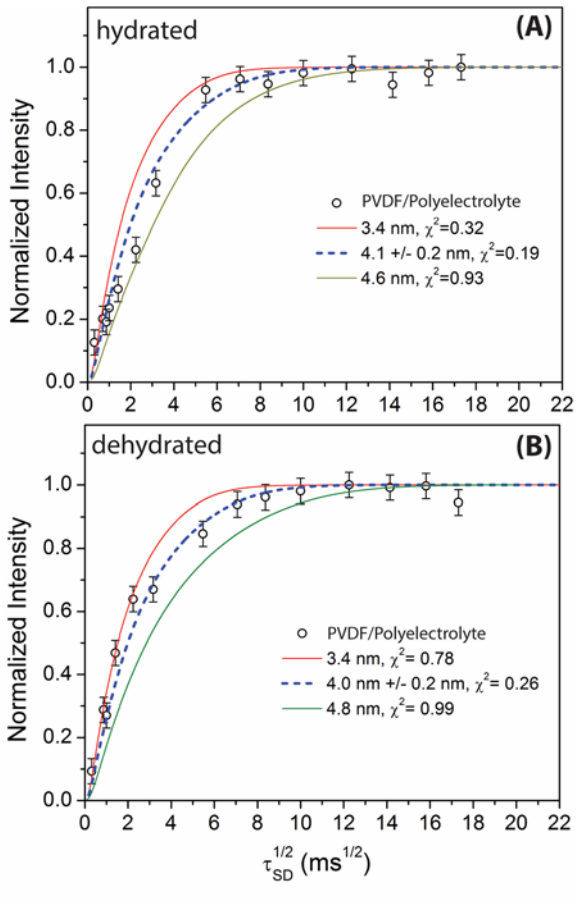

Figure 4: NMR spin diffusion magnetization recovery curves obtained from the ^{1}H-detected ^{1}H-^{19}F REDOR-filtered pulse sequence (Figure 1A). Experimental data points are the integrated intensities of the ^{1}H resonance of the PVDF domain as a function of $\sqrt{\tau_{SD}}$. Best fit simulations (broken lines) obtained by numerically solving the Equation (3) to minimize χ^2 using a 3D model of isolated dispersed PVDF domains as discussed in the text. Solid lines show the behavior of simulations with smaller (top) and larger (bottom) domain sizes.

Simulation assuming a 3D uniform-sized domain model again estimates an average PVDF domain size of 4.1 ±0.1 nm (^{13}C CP detected), and agrees with the size measured from the direct ^{1}H observation NMR spin diffusion experiment (Figure 4A). While the S/N in this example is low, the resulting spin diffusion recovery curve remains well-behaved due to the improved spectral resolution afforded in the ^{13}C NMR spectra. By including a final ^{1}H-^{19}F CP step, it is also possible to monitor the ^{1}H spin diffusion through detection of the ^{19}F in the PVDF domain. This CP step takes advantage of the increased sensitivity and high natural abundance of the ^{19}F nucleus along with avoiding potential complications from overlapping ^{13}C resonances. The ^{19}F NMR spectra for the dehydrated polymer blend following a ^{1}H-^{19}F REDOR-filtered spin diffusion experiments is shown in Figure 5C. Here, the entire ^{19}F MAS NMR spectrum (including spinning side bands) is integrated to generate the recovery curve shown in Figure 5D. PVDF

exists in a mixture of amorphous and crystalline phases which manifest different chemical shifts, complicating what might otherwise be expected to be a simple spectrum. The different ^{19}F assignments were made using a crystalline filtering experiment (see supplemental material) and match previous literature assignments.[33] We argue that for this blend these NMR spin diffusion experiments are probing the morphology of a mixed phase, and that for this polymer blend large PVDF crystallites are not present. The characteristic ^{19}F resonances associated with the formation of the β form PVDF crystallites was not observed except for blends where clear μm phase separation is seen in the SEM (additional discussion in supplemental). The domain size of this mixed phase was estimated to be 4.0 ±0.1 nm, and matches the measurements obtained with the other pulse sequences variations described above. The ^{19}F-^{1}H REDOR sequence with short dephasing periods ($N_C \sim 6$) selectively dephases the PVDF crystalline resonances in the ^{19}F NMR since the ^{1}H-^{19}F heteronuclear dipolar coupling is stronger in the crystalline versus amorphous phase, and has been used to measure the degree of crystallinity in PVDF by Ando and co-workers.[33] In principal, this dephasing difference could be used to measure the relative domain size of the crystalline and amorphous phases of PVDF by monitoring ^{19}F spin diffusion between these domains, but were not pursued in the current study as we are probing the morphology of a mixed phase with no significant-sized crystallites. In addition, even if there were distinct amorphous and crystalline phases on the nm scale in these blends, the NMR spin diffusion experiments would be further complicated by both the aromatic and amorphous PVDF contributing to the source magnetization. It is also possible to extend the ^{1}H-^{19}F REDOR-filtered NMR spin diffusion pulse sequences presented here to other nuclei for measuring domain sizes in heterogeneous material, if there are unique spin pairs associated with a given phase (of sufficient natural or enriched abundance) that allows dephasing through the heteronuclear dipolar coupling. Other examples might include ^{1}H-^{31}P, ^{19}F-^{31}P, ^{1}H-^{7}Li, ^{1}H-^{2}H, ^{31}P-^{23}Na REDOR filtered NMR spin diffusion experiments, and would depend on the specific material of interest.

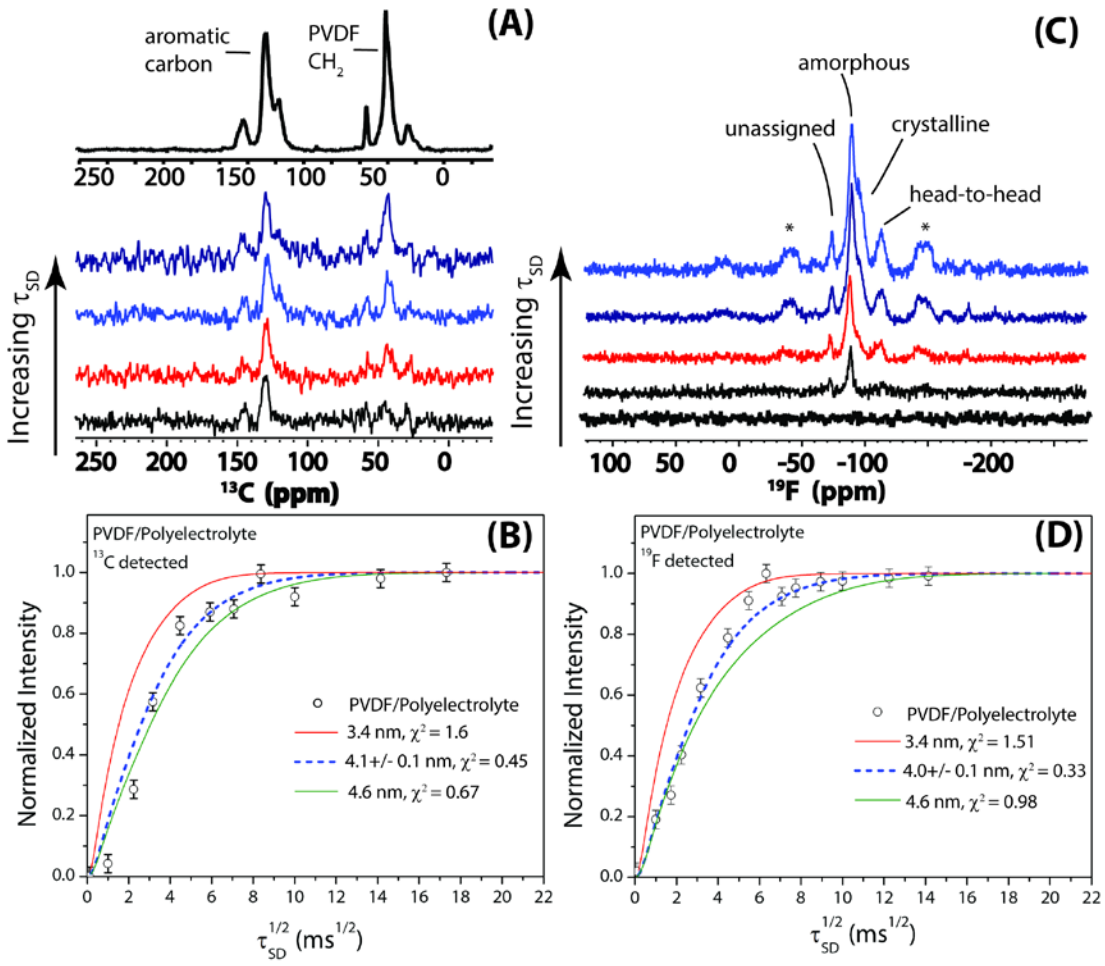

Figure 5: ^{1}H-^{19}F REDOR-filtered NMR spin diffusion data for the (A) ^{1}H→^{13}C CP detected pulse sequence (Figure 1B) and the (C) ^{1}H→^{19}F CP detected pulse sequence (Figure 1C). The spin diffusion recovery curves (B and D) show the experimental data (open symbols) along with simulated response curves (dashed and solid lines) based on Eqn. (3) for different PVDF domain sizes. Additional simulation details are provided in the text.

While based on the heteronuclear REDOR sequence, the methods presented above differ from the ^{1}H-^{13}C "hole-burning" technique presented by Schmidt-Rohr.[36] For the PVDF polymer blend sample, the fluorinated domains have high ^{19}F densities, such that the description of an isolated nucleus (^{13}C in Ref. 36) dephasing the surrounding ^{1}H bath is not applicable. Rather, the ^{19}F and ^{1}H nuclei, of roughly equal number densities, are dipolar-coupled in the PVDF domain with the REDOR filter dephasing of the entire domain. The presence of these strong multi-spin interactions precludes an estimate of the upper domain size that can be studied using these ^{1}H-^{19}F REDOR-filtered NMR spin diffusion experiments (beyond the T_1 relaxation time limitation discussed in the previous sections). However, we note that NMR spin diffusion techniques described in this work probe length scales below the resolution limit of traditional microscopy techniques such as SEM or TEM in polymers, and furthermore require no electron density con-

trast. For the polymer blend sample characterized in this work, separate chemical domains were not visible, with the sample appearing completely homogeneous in SEM images (see Figure 1A of Ref. 40).[40] For polymer blend samples where distinct μm-sized domains were evident in SEM (see Figure 1B and 1C of Ref. 40), the polyelectrolyte and PVDF are no longer mixed at the molecular level and have significantly reduced interfaces between the different polymers, such that the NMR spin diffusion experiments were not successful.

Conclusions

We have demonstrated a ^{1}H-^{19}F REDOR–filtered NMR spin diffusion pulse sequence allowing the selective suppression of the ^{1}H signal originating in fluorinated polymer domains. This sequence was used to measure the domain size of PVDF within a blended copolymer currently being considered for use as a proton exchange membrane in fuel cells. It is shown that through both direct ^{1}H detection along with ^{1}H-^{13}C and ^{1}H-^{19}F CP detection of the NMR ^{1}H spin diffusion process, consistent measurements of the domain size were obtained. Provided that the domain of interest contains a unique heteronuclear spin pair, these types of REDOR-filtered NMR spin diffusion experiments could be used to selectively suppress magnetization in that domain using the corresponding heteronuclear dipolar dephasing. This class of REDOR-filtered NMR spin diffusion pulse sequences provide an additional tool for probing domain sizes in heterogeneous materials where other magnetization filtering technique prove insufficient.

Acknowledgements

Sandia National Laboratories is a multi-mission laboratory managed and operated by National Technology and Engineering Solutions of Sandia, LLC., a wholly owned subsidiary of Honeywell International, Inc., for the U.S. Department of Energy's National Nuclear Security Administration under contract DE-NA-0003525. This work was funded by the Sandia LDRD program. The authors gratefully acknowledge Prof. Louis A. Madsen and Arkema Inc. for providing the blended copolymer membranes for demonstration of this sequence.

References

[1] F. Hussain, M. Hojjati, M. Okamoto, R. E. Gorga, *J. Compos. Mater.* **2006**, *40*, 1511-1575.
[2] A. Gruger, A. Régis, T. Schmatko, P. Colomban, *Vib. Spectrosc* **2001**, *26*, 215-225.
[3] M. McCormick, R. N. Smith, R. Graf, C. J. Barrett, L. Reven, H. W. Spiess, *Macromolecules* **2003**, *36*, 3616-3625.
[4] B. Smitha, S. Sridhar, A. Khan, *J. Membr. Sci.* **2003**, *225*, 63-76.
[5] T. A. Zawodzinski Jr, M. Neeman, L. O. Sillerud, S. Gottesfeld, *J. Phys. Chem.* **1991**, *95*, 6040-6044.
[6] F. Wang, M. Hickner, Y. S. Kim, T. A. Zawodzinski, J. E. McGrath, *J. Membr. Sci.* **2002**, *197*, 231-242.
[7] H.-G. Haubold, T. Vad, H. Jungbluth, P. Hiller, *Electrochim. Acta* **2001**, *46*, 1559-1563.

[8] S. J. Paddison, R. Paul, *PCCP* **2002**, *4*, 1158-1163.
[9] A.-L. Rollet, O. Diat, G. Gebel, *J. Phys. Chem. B* **2002**, *106*, 3033-3036.
[10] S. K. Young, S. Trevino, N. C. Beck Tan, *J. Polym. Sci., Part B: Polym. Phys.* **2002**, *40*, 387-400.
[11] F. Barbir, in *Fuel Cell Technology*, Springer, **2006**, pp. 27-51.
[12] J. Zhang, Z. Xie, J. Zhang, Y. Tang, C. Song, T. Navessin, Z. Shi, D. Song, H. Wang, D. P. Wilkinson, *J. Power Sources* **2006**, *160*, 872-891.
[13] H. Lee, M. Yanilmaz, O. Toprakci, K. Fu, X. Zhang, *Energy & Environmental Science* **2014**, *7*, 3857-3886.
[14] L. J. Small, H. D. Pratt, C. H. Fujimoto, T. M. Anderson, *J. Electrochem. Soc.* **2016**, *163*, A5106-A5111.
[15] R. L. Weber, Y. Ye, A. L. Schmitt, S. M. Banik, Y. A. Elabd, M. K. Mahanthappa, *Macromolecules* **2011**, *44*, 5727-5735.
[16] Y. A. Elabd, M. A. Hickner, *Macromolecules* **2010**, *44*, 1-11.
[17] M. A. Hickner, H. Ghassemi, Y. S. Kim, B. R. Einsla, J. E. McGrath, *Chem. Rev.* **2004**, *104*, 4587-4612.
[18] H.-S. Lee, A. Roy, O. Lane, S. Dunn, J. E. McGrath, *Polymer* **2008**, *49*, 715-723.
[19] N. Bloembergen, *Physica* **1949**, *15*, 386-426.
[20] K. Schmidt-Rohr, H. Spiess, *Multidimensional Solid-State NMR and Polymers*, AP Inc., Mainz, Germany, **1994**.
[21] P. Caravatti, M. Levitt, R. Ernst, *J. Magn. Reson.* **1986**, *68*, 323-334.
[22] P. Caravatti, P. Neuenschwander, R. Ernst, *Macromolecules* **1985**, *18*, 119-122.
[23] J. R. Havens, D. L. VanderHart, *Macromolecules* **1985**, *18*, 1663-1676.
[24] J. Clauss, K. Schmidt-Rohr, H. W. Spiess, *Acta Polym.* **1993**, *44*, 1-17.
[25] R. Assink, *Macromolecules* **1978**, *11*, 1233-1237.
[26] I. J. Colquhoun, K. J. Packer, *Br. Polym. J.* **1987**, *19*, 151-163.
[27] T. Kimura, K. Neki, N. Tamura, F. Horii, M. Nakagawa, H. Odani, *Polymer* **1992**, *33*, 493-497.
[28] K. Packer, J. Pope, R. Yeung, M. Cudby, *J. Polym. Sci., Polym. Phys. Ed.* **1984**, *22*, 589-616.
[29] K. Schmidt-Rohr, J. Clauss, B. Blümich, H. W. Spiess, *Magn. Reson. Chem.* **1990**, *28*, S3-S9.
[30] B. R. Cherry, C. H. Fujimoto, C. J. Cornelius, T. M. Alam, *Macromolecules* **2005**, *38*, 1201-1206.
[31] T. M. Alam, J. U. Otaigbe, D. Rhoades, G. P. Holland, B. R. Cherry, P. G. Kotula, *Polymer* **2005**, *46*, 12468-12479.
[32] T. Cheung, B. Gerstein, *J. Appl. Phys.* **1981**, *52*, 5517-5528.
[33] S. Ando, R. K. Harris, U. Scheler, *Fluorine-19 NMR of Solids Containing Both Fluorine and Hydrogen, Vol. 9*, John Wiley & Sons, Ltd., Chichester, **2002**.
[34] K. Schmidt-Rohr, J. Clauss, H. Spiess, *Macromolecules* **1992**, *25*, 3273-3277.
[35] K. Schmidt-Rohr, A. Rawal, X.-W. Fang, *J. Chem. Phys.* **2007**, *126*, 054701/054701 - 054701/054716.
[36] Q. Chen, K. Schmidt-Rohr, *Solid State Nucl. Magn. Reson.* **2006**, *29*, 142-152.
[37] K. Schäler, M. Roos, P. Micke, Y. Golitsyn, A. Seidlitz, T. Thurn-Albrecht, H. Schneider, G. Hempel, K. Saalwächter, *Solid State Nucl. Magn. Reson.* **2015**, *72*, 50-63.
[38] M. Roos, P. Micke, G. Hempel, *Chem. Phys. Lett.* **2012**, *536*, 147-154.
[39] M. Roos, P. Micke, K. Saalwächter, G. Hempel, *J. Magn. Reson.* **2015**, *260*, 28-37.
[40] J. Hou, J. Li, D. Mountz, M. Hull, L. A. Madsen, *J. Membr. Sci.* **2013**, *448*, 292-299.
[41] D. Massiot, F. Fayon, M. Capron, I. King, S. Le Calvé, B. Alonso, J. O. Durand, B. Bujoli, Z. Gan, G. Hoatson, *Magn. Reson. Chem.* **2002**, *40*, 70-76.
[42] T. Gullion, J. Schaefer, *J. Magn. Reson.* **1989**, *81*, 196-200.
[43] E. L. Hahn, *Phys. Rev.* **1950**, *80*, 580-594.
[44] T. Gullion, *Concepts Magn. Reson.* **1998**, *10*, 277-289.
[45] T. Gullion, *Modern Magnetic Resonance: Rotational-Echo, Double-Resonance NMR*, Springer, **2008**.
[46] M. Bertmer, H. Eckert, *Solid State Nucl. Magn. Reson.* **1999**, *15*, 139-152.
[47] T. Echelmeyer, L. van Wüllen, S. Wegner, *Solid State Nucl. Magn. Reson.* **2008**, *34*, 14-19.
[48] E. G. Sorte, Lauren J. Abbott, Mark Wilson, Amalie Frischknecht, and Todd M. Alam, *J. Polym. Sci., Part B: Polym. Phys.* **2017**, *submitted*.
[49] J. Crank, *The Mathematics of Diffusion*, Oxford University Press, **1979**.
[50] D. E. Demco, A. Johansson, J. Tegenfeldt, *Solid State Nucl. Magn. Reson.* **1995**, *4*, 13-38.
[51] T. Cheung, B. Gerstein, L. Ryan, R. Taylor, D. Dybowski, *J. Chem. Phys.* **1980**, *73*, 6059-6067.
[52] P. Holstein, G. Monti, R. Harris, *PCCP* **1999**, *1*, 3549-3555.
[53] M. E. Halse, A. Zagdoun, J.-N. Dumez, L. Emsley, *J. Magn. Reson.* **2015**, *254*, 48-55.
[54] Z. Jia, L. Zhang, Q. Chen, E. Hansen, *J. Phys. Chem. A* **2008**, *112*, 1228-1233.
[55] A. Krushelnitsky, T. Bräuniger, D. Reichert, *J. Magn. Reson.* **2006**, *182*, 339-342.